Eur. Phys. J. B **54**, 267–273 (2006)
DOI: 10.1140/epjb/e2006-00449-5

THE EUROPEAN PHYSICAL JOURNAL B

The effects of reaction delay in the Nagel-Schreckenberg traffic flow model

R. Jiang[1,a], M.B. Hu[1], B. Jia[2], R.L. Wang[3], and Q.S. Wu[1]

[1] School of Engineering Science, University of Science and Technology of China, Hefei 230026, P.R. China
[2] School of Traffic and Transportation, Beijing Jiaotong University, Beijing 100044, P.R. China
[3] Institute of Information Sciences and Technology, Massey University, Private Bag 11-222, Palmerston North, New Zealand

Received 27 August 2006
Published online 22 December 2006 –

Abstract. This paper studies a new model, which considers the effects of drivers reaction delay in the Nagel-Schreckenberg model. We studied the traffic flow properties in the new model under both periodic and open boundary conditions. The fundamental diagram, spatio-temporal patterns, density-density correlation functions, relaxation time, and distance headway distribution are investigated. Several interesting results are reported, for example, (i) the jam becomes less condensed when the delay effect is considered; (ii) the distance headway of the new model exhibits a multi-peak distribution when randomization p is small; (iii) for large p, the distribution of distance headway follows a power law in the new model; (iv) under open boundary conditions, the existence of a stationary jam near the left boundary will lower the flow rate.

PACS. 89.40.-a Transportation

1 Introduction

Recently the traffic flow problem has attracted the interests of many physicists and engineers [1–5]. There are two different conceptual frameworks for modeling traffic. In the "coarse-grained" fluid-dynamical description traffic is viewed as a compressible fluid formed by vehicles, but these individual vehicles do not appear explicitly in the theory. In contrast, in the so-called "microscopic" vehicular traffic flow models, attention is explicitly focused on individual vehicles; the nature of the interactions among these vehicles is determined by the way in which the vehicles influence each others' movement.

Microscopic models can be further classified into so-called car-following models and cellular automata (CA) models. In the car-following models [6–8], one writes for each individual vehicle an equation of motion which is the analogue of Newton's equation for each individual particle in a system of interacting classical particles. In the earliest car-following models [9] the difference in the velocities of the nth and $(n+1)$th vehicles was assumed to be the stimulus for the nth vehicle to change its speed. In other words, it was assumed that every driver tends to move with the same speed as that of the corresponding leading vehicle so that

$$\frac{dv_n}{dt}(t) = \kappa(v_{n+1}(t) - v_n(t)), \tag{1}$$

where κ is a sensitivity coefficient. Later it has been argued [10] that, for a more realistic description, the strength of the response of a driver at time t should depend on the stimulus received from the other vehicles at time $t-T$, where T is the reaction delay time of the drivers. Therefore, generalizing equation (1), one would get

$$\frac{dv_n}{dt}(t) = \kappa(v_{n+1}(t-T) - v_n(t-T)). \tag{2}$$

Studies show that T is a very important parameter, for example, (i) if $\kappa T > \pi/2$, the solution of equation (2) is oscillatory with increasing amplitude; (ii) if $\kappa T = \pi/2$, the solution is oscillatory with constant amplitude; (iii) if $1/e < \kappa T < \pi/2$, the solution is oscillatory with damped amplitude; (iv) if $\kappa T \leq 1/e$, the solution is non-oscillatory and damped [11,12].

In 1995, Bando et al. proposed the well-known optimal velocity (OV) model [13], and it is shown that the model could describe such traffic phenomenon as stop-and-go waves. Later, the reaction delay effect was also taken into account in the OV model [14,15]. Moreover, Del Castillo et al. also studied the reaction times of drivers and the stability of traffic flow [16].

Recently, modelling road traffic behavior using cellular automata (CA) has become a well-established method to model, analyze, understand and even forecast the behavior of real road traffic because the automatas evolution rules are simple, straightforward to understand, computationally efficient and sufficient to emulate much of the behavior of observed traffic flow [3–5,17]. Since the

[a] e-mail: rjiang@ustc.edu.cn

Nagel-Schreckenberg (NaSch) model [18] was proposed in 1992, various CA models have been proposed [1–5,17]. These models are successful in reproducing many traffic features such as stop-and-go waves, metastable states, synchronized flow, capacity drop and so on.

Nevertheless, in these CA models, the reaction delay time of drivers has not been considered (at least not explicitly considered). Therefore, in this paper, we incorporate the delay time into the NaSch model and investigate the delay effects in CA models.

The paper is organized as follows. In the next section, the NaSch model is revised to take the delay time into account. The simulation results are presented and compared in Section 3. The conclusions and outlook are given in Section 4.

2 The NaSch model considering delay time

In this section, we briefly recall the definition of the NaSch model first. The NaSch model is a discrete model for traffic flow. A road is divided into cells, which can be either empty or occupied by a vehicle with a velocity $v = 0, 1, ..., v_{max}$. The vehicles move from the left end of a road to the right end of the road. At each discrete time step $t \to t+1$, the system update is performed in parallel according to the following four sub-rules:

1. acceleration: $v_n(t+\frac{1}{3}) \to \min(v_n(t)+1, v_{max})$;
2. deceleration: $v_n(t+\frac{2}{3}) \to \min(v_n(t+\frac{1}{3}), d_n(t))$;
3. randomization: $v_n(t+1) \to \max(v_n(t+\frac{2}{3})-1, 0)$ with probability p;
4. position update: $x_n(t+1) \to x_n(t) + v_n(t+1)$.

Here, v_n and x_n denote the velocity and position of the vehicle n respectively; v_{max} is the maximum velocity and $d_n = x_{n+1} - x_n - 1$ denotes the number of empty cells in front of the vehicle n; p is the randomization probability.

If we combine steps 1 and 2 together, we have

$$v_n\left(t+\frac{2}{3}\right) \to \min(v_n(t)+1, d_n(t), v_{max}).$$

This means the acceleration of the vehicle (without considering the randomization) is

$$A(t) = \min(v_n(t)+1, d_n(t), v_{max}) - v_n(t). \quad (3)$$

If we consider the delay effect (the delay time is set to one time step, i.e., 1 s, in this paper), the acceleration needs to be changed to

$$A(t) = \min(v_n(t-1)+1, d_n(t-1), v_{max}) - v_n(t-1). \quad (4)$$

Therefore, a modified NaSch Model considering delay time (here referred to as NaSch-D model) are listed as follows:

1. determination of acceleration: $A(t) = \min(v_n(t-1)+1, d_n(t-1), v_{max}) - v_n(t-1)$;
2. adjustment of velocity: $v_n(t+\frac{2}{3}) \to \min(v_n(t)+A(t), d_n(t), v_{max})$;
3. randomization: $v_n(t+1) \to \max(v_n(t+\frac{2}{3})-1, 0)$ with probability p;
4. position update: $x_n(t+1) \to x_n(t) + v_n(t+1)$.

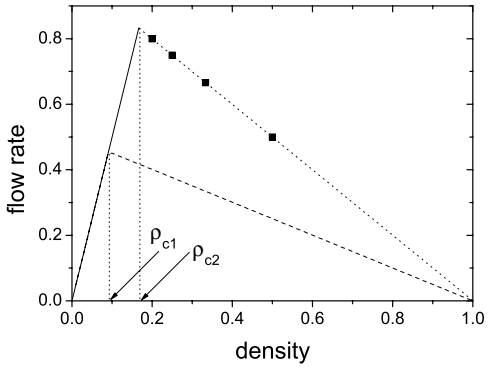

Fig. 1. The fundamental diagram of deterministic NaSch-D model. The dotted line shows the congested branch of the deterministic NaSch model.

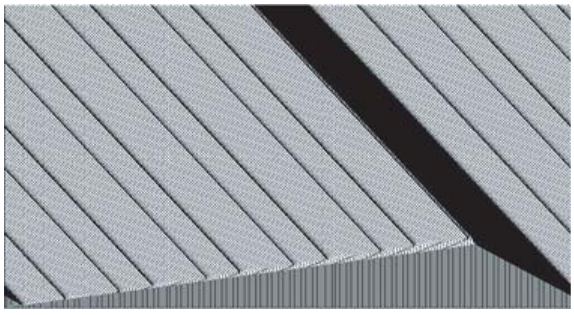

Fig. 2. The evolution of a disturbance in the homogeneous traffic flow. The road length is $L = 1000$. Initially there are 200 vehicles, which are homogeneously distributed. Then one vehicle is removed from the system.

3 Simulation results

In this section, the numerical investigation of the NaSch-D model is carried out and compared with the results of the NaSch model. The maximum velocity is set to $v_{max} = 5$. The system size is $L = 1000$ unless otherwise mentioned. Periodic boundary conditions and open boundary conditions are adopted respectively in the following two subsections.

3.1 Periodic boundary conditions

Firstly we consider the deterministic version of the NaSch-D model (i.e., the randomization p is set to 0). Figure 1 shows the fundamental diagram of the deterministic NaSch-D model. One can see that two branches as well as four scattered points exist. The solid line branch and the scattered points are from the homogeneous initial configuration and the dashed line branch is from the random initial configuration. The four scattered points fall on the right branch of the fundamental diagram, but any small disturbance will destroy the homogeneity of the traffic flow and the traffic flow will lower to the dashed line branch (for example, see Fig. 2). Therefore, these states are unstable.

For the solid line branch in density range $\rho_{c1} < \rho < \rho_{c2}$, a small disturbance will dissipate with time but a

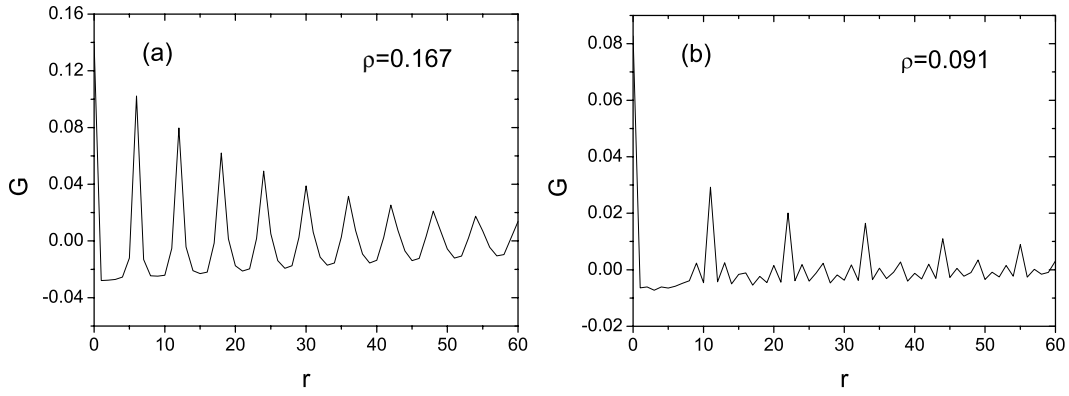

Fig. 3. The density-density correlation function in (a) the NaSch model (b) the NaSch-D model. The density corresponds to critical density in the NaSch model and critical density ρ_{c1} in the NaSch-D model. The initial configuration is random in both cases.

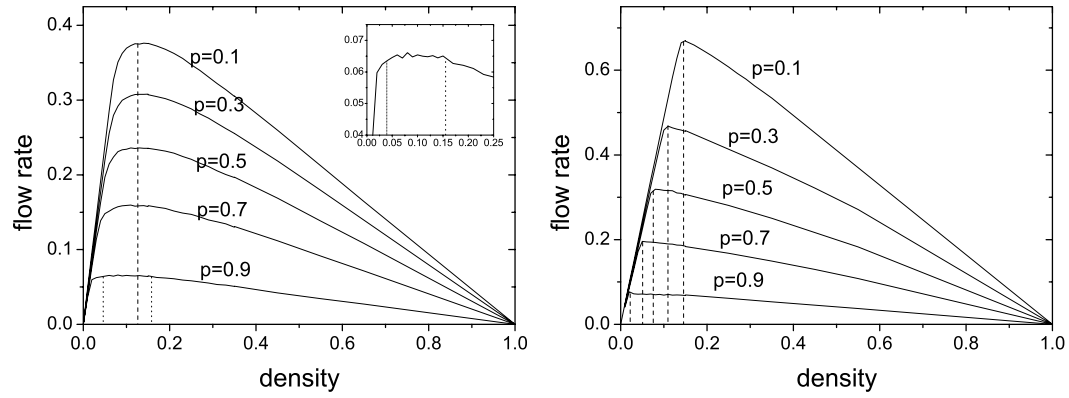

Fig. 4. (a) The fundamental diagram of the non-deterministic NaSch-D model. The inset shows the details between the two dotted lines. (b) The fundamental diagram of the non-deterministic NaSch model. In (b), the system $L = 10\,000$ is used to avoid the finite size effect.

large disturbance will reduce the traffic flow to the dashed line branch. The critical amplitude of the disturbance decreases with the increase of density and tends to zero at ρ_{c2}. Therefore, these states are metastable.

For the dashed line branch, the traffic flow is a mixture of free flow and jams (Fig. 2). The flow rate corresponding to ρ_{c1} is the flow rate out of jams and ρ_{c1} its corresponding density. Considering two vehicles in jams, when the first vehicle begins to accelerate, the second vehicle will accelerate two time steps later due to time delay. As a result, when both vehicles reach maximum velocity, the net distance between two vehicles is 10 cells. Consequently, $\rho_{c1} = 1/11 = 0.0909$ and the corresponding flow rate is 0.4545. The numerical results are in very good agreement with the analysis.

Figure 3 compares the density-density correlation function, which is defined as

$$G(r) = \frac{1}{\tau}\frac{1}{L}\sum_{t=1}^{\tau}\sum_{j=1}^{L} n_j n_{j+r} - \rho,$$

in the NaSch model and NaSch-D model. Here $n_j = 0$ for an empty cell and $n_j = 1$ for a cell occupied by a vehicle. One can see that the interval between the peaks is much larger in the NaSch-D model than in the NaSch model. This is because in the NaSch-D model, the net distances between two successive vehicles are normally larger than or equal to 10 cells due to the delay effect.

Next we investigate the randomization effect in the NaSch-D model. Figure 4a shows the fundamental diagram of the non-deterministic NaSch-D model. The metastable states existing in the deterministic NaSch-D model disappear due to the randomization effect (see, Fig. 5).

Compared with the fundamental diagram of the NaSch model (Fig. 4b), it can be seen that the flow rate exhibits a smooth variation at its maximum value. Moreover, the maximum flow rate is lower in the NaSch-D model than in the NaSch model. This means that the reaction delay of drivers will decrease the capacity of a road. The capacity difference is large for small p. However, with the increase of p, the difference decreases. When p is large, the difference becomes small (Fig. 6).

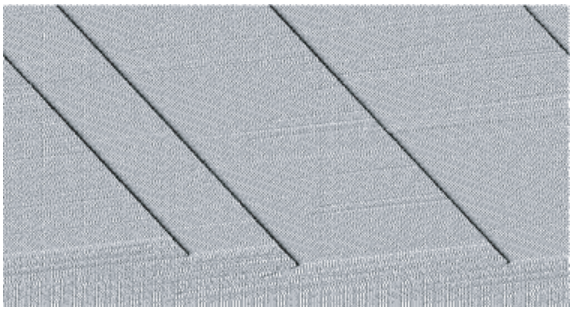

Fig. 5. The appearance of jams from homogeneous traffic. The density $\rho = 0.1$ is only slightly larger than $\rho_{c1} = 0.0909$, and the randomization $p = 0.01$. One can see that even with such a small randomization effect, the jams appear very quickly (in about 100 time steps).

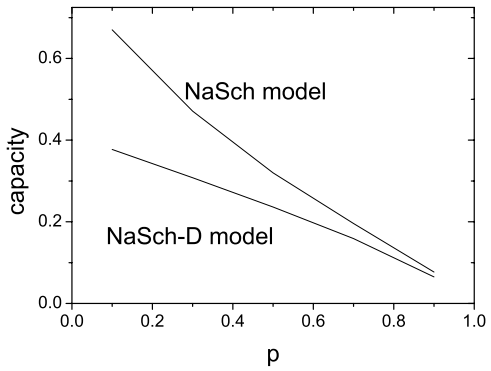

Fig. 6. The capacity of the NaSch model and NaSch-D model.

We also notice that in the NaSch model, the density corresponding to maximum flow rate decreases with the increase of p (dashed lines in Fig. 4b). But, in NaSch-D model, this density is essentially independent of the value of p (the dashed line in Fig. 4a). Furthermore, when p is very large ($p = 0.9$), a rough plateau forms in the density range between the two dotted lines.

Note that in systems with ramps and systems with a stationary defect, a plateau formation will be exhibited in the fundamental diagram. In the disordered model proposed in [19], a plateau in the fundamental diagram is induced by the 'careless' drivers (dynamic defects) that act as blockages in a system. Our model, therefore, is different since it leads to a plateau under its intrinsic dynamics without introducing any static and dynamic artificial defects.

Figure 7 compares the spatio-temporal structures of the NaSch-D model and the NaSch model. One can see that the spatio-temporal features of the NaSch-D model are quite different from those of the NaSch model: the jams are more condensed in the NaSch model. In other words, the reaction delay of drivers spreads the jams over the road. This is also manifested from the distance headway distribution as shown in Figure 8, where the distribution of the NaSch model is narrower than that in the NaSch-D model.

More interestingly, the distance headway of the NaSch-D model exhibits a multi-peak distribution when randomization p is small. These peaks correspond to distance headway 1, 4, 6, 8, 10 respectively. Except for the first peak, the difference between other headways corresponding to the peaks is 2. This is because, when accelerating from a jam, the second vehicle will be delayed for two time steps. When the second vehicle begins to accelerate, it is usually two cells behind the first vehicle.

Furthermore, we also notice that the probability that distance headway is 1 only slightly depends on p in the NaSch-D model (while in the NaSch model, it increases with the increase of p). This means that with the increase of p, the number of jammed (or stopped) vehicles only slightly increases, but more vehicles have to slow down. This explains why spatio-temporal structures of the NaSch-D model are different from those of the NaSch model.

With the increase of p, the multi-peaks distribution in NaSch-D model is smeared. Moreover, we find that for large p, the distribution of distance headway follows a power law in NaSch-D model, while it deviates the power law in NaSch model. This implies that with the consideration of reaction delay of drivers, the self-organized criticality (SOC), which is observed in real traffic [20,21], can be depicted.

We also compare the relaxation time, which is characterized by the parameter

$$\tau = \int_0^\infty [\min\{v^*(t), < \bar{v}_\infty >\} - < \bar{v}(t) >]dt$$

in the NaSch-D model and NaSch model. Here $v^*(t)$ denotes the average velocity in the acceleration phase $t \to 0$ for low vehicle density $\rho \to 0$. In this regime, due to the absence of interactions between the vehicles, one has $v^*(t) = (1-p)t$. We start from a random configuration of vehicles with velocity $v_j = 0$, the average velocity $\bar{v}(t)$ is measured at each time step t. For $t \to \infty$, the system reaches a stationary state with average velocity $\bar{v}_\infty$. Figure 9 shows that the maximum of the relaxation parameter is near, but below, the density corresponding to maximum flow (cf. Fig. 4) in both models. However, in the NaSch model, τ decreases quickly when the maximum is reached while it decreases relatively slowly in the NaSch-D model. This may indicate that the transitions from free flow to congested flow in these two models are qualitatively different, which will be further explored in our future work.

3.2 Open boundary conditions

For open boundary conditions, vehicles enter a road from the left end of the road and move out of the road from the right end. At an entry, a new vehicle is inserted at $x_{in} = \min[2v_{max} + 1, x_{last} - (v_{max} + 1)]$ with maximum velocity v_{max} with probability α when the last vehicle is beyond $2v_{max} + 1$ (i.e.,$x_{last} > 2v_{max} + 1$). For the NaSch-D model, it is assumed that its velocity is v_{max} in the

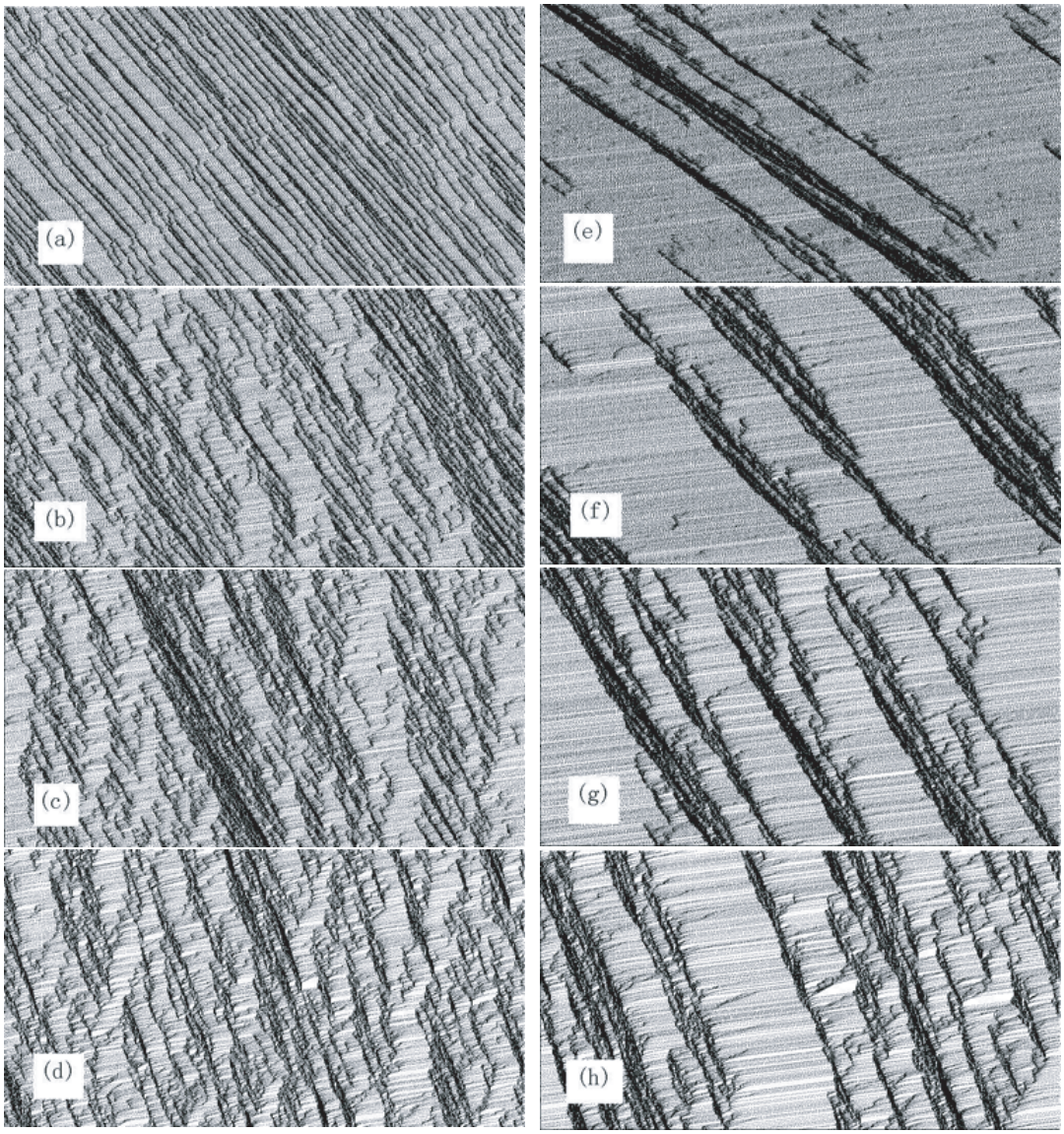

Fig. 7. The spatio-temporal structures of the NaSch-D model and the NaSch model. (a–d) show those of NaSch-D model and (e–h) show those of NaSch model. The randomization is $p = 0.1$ in (a, e), $p = 0.3$ in (b, f), $p = 0.5$ in (c, g), $p = 0.7$ in (d, h).

previous time step. Therefore, its position in the previous step is $x_{in} - v_{max}$. At the right boundary, a vehicle is removed when it is beyond L. Furthermore, a speed limit region is imposed between $0.7L$ and $0.8L$, in which the maximum velocity reduces to $v_{max,limit}$.

Similarly, we consider the deterministic version of the NaSch-D model first. Figure 10 shows the dependence of the flow rate on the entrance probability α in the NaSch-D model without consideration of the speed limit. The flow rate increases monotonically with α. Furthermore, the flow rate is identical with that of the deterministic NaSch model.

When considering the speed limit, some interesting results are identified. Figure 11 shows the dependence of the flow rate on the entrance probability α where $v_{max,limit} = 2$ and 3. One can see that in the NaSch-D model, the flow rate firstly increases with α. After the maximum is reached, it begins to decrease with α. This is different from the NaSch model, where after the maximum is reached, the constant flow rate is maintained.

Figure 12 shows the spatio-temporal patterns of the NaSch-D model at two different values of α. One can see that the patterns are different from each other. When $\alpha = 1$, the density waves are identical to each other, while this is not the case for $\alpha = 0.5$. We notice that for $\alpha = 1$, a stationary jam exists near the left boundary,and this lowers the flow rate.

Next we investigate the randomization effect in open boundary conditions. Figure 10 also shows the dependence of the flow rate on the entrance probability α in the non-deterministic NaSch-D model (without consideration of speed limit). One can see that for small p, the flow rate first increases then decreases with α. With the increase of p, the phenomenon gradually weakens. When p

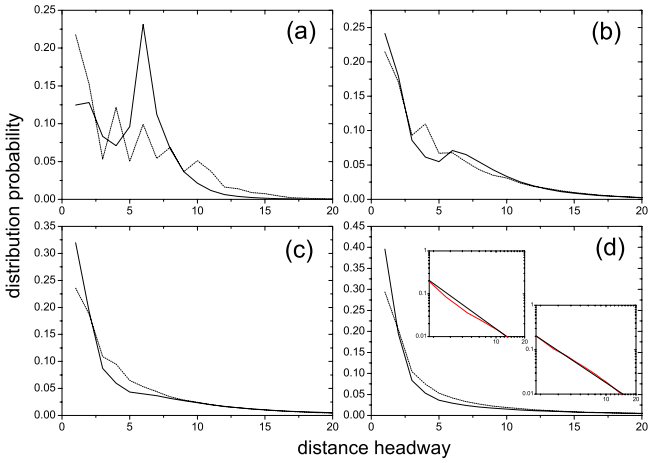

Fig. 8. (Color online) The distance headway distribution in the NaSch-D model (dashed lines) and in the NaSch model (solid lines). The density $\rho = 0.2$. (a) $p = 0.1$; (b) $p = 0.3$; (c) $p = 0.5$; (d) $p = 0.7$. In (d), the left inset (red line) shows the distribution of the NaSch model in a log-log plane, the right inset (red line) shows the distribution of the NaSch-D model in a log-log plane. The black lines in both insets are straight lines for guidance of these.

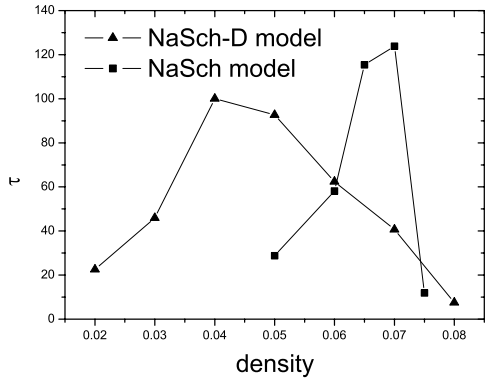

Fig. 9. The relaxation parameter near the transition density. The system size used is $L = 200\,000$, the randomization $p = 0.5$.

is large, the flow rate remains constant after the maximum is reached.

Figure 13 shows the spatio-temporal patterns of the non-deterministic NaSch-D model at two different values of α. As mentioned before, it is evident that a stationary jam exists near the left boundary for $\alpha = 1$. This lowers the flow rate. With the increase of p, the stationary jam is gradually broken. Therefore, the flow rate can remain constant after the maximum is reached.

4 Conclusion

This paper has investigated the effects of drivers reaction delay in the Nagel-Schreckenberg (NaSch) model. The acceleration rule in the NaSch model is revised to incorporate delay time, so we have used a NaSch-D model.

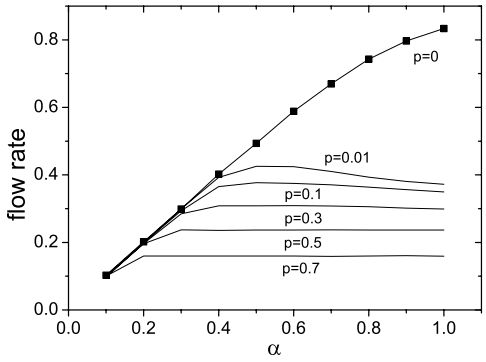

Fig. 10. The dependence of the flow rate on the entrance probability α in the NaSch-D model. The scattered data shows the flow rate of the deterministic NaSch model.

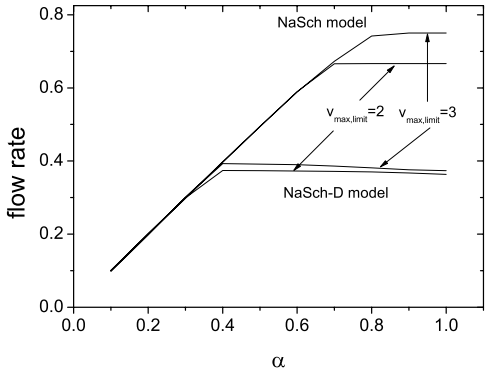

Fig. 11. The dependence of the flow rate on the entrance probability α in the NaSch-D model and NaSch model.

We studied traffic flow properties in the NaSch-D model under both periodic and open boundary conditions. The fundamental diagram, spatio-temporal patterns, density-density correlation functions, relaxation time, and distance headway distribution are investigated.

Results found are as follows: (i) the metastable state exists in the deterministic NaSch-D model; (ii) the interval between the peaks in the density-density correlation function is much larger in the NaSch-D model than that in the NaSch model; (iii) the reaction delay of drivers will decrease the capacity of a road; (iv) a rough plateau forms in the fundamental diagram when p is large; (v) the jams are more condensed in NaSch model than in NaSch-D model; (vi) the distance headway of NaSch-D model exhibits a multi-peak distribution when randomization p is small; (vii) for large p, the distribution of distance headway follows a power law in NaSch-D model; (viii) under open boundary conditions, the existence of a stationary jam near the left boundary will lower the flow rate.

In future work, we will extend the NaSch-D model to multi-lane roads and study the delay effects in lane changing behaviors. Furthermore, the delay effects in other cellular automata traffic flow models, such as the models that can describe synchronized flow, will also be investigated.

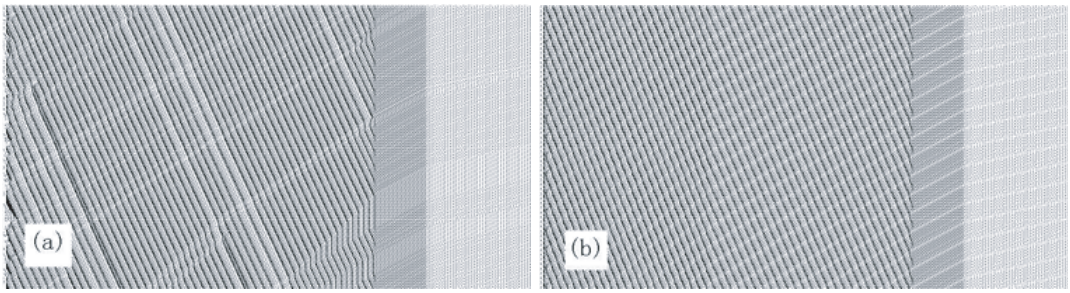

Fig. 12. The spatio-temporal patterns of the deterministic NaSch-D model at two different values of α. (a) $\alpha = 0.5$; (b) $\alpha = 1.0$. The parameter $v_{max,limit} = 2$.

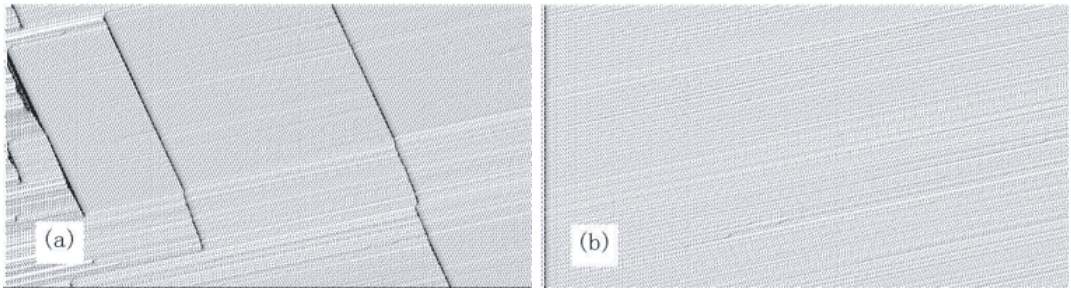

Fig. 13. The spatio-temporal patterns of the non-deterministic NaSch-D model at two different values of α. (a) $\alpha = 0.5$; (b) $\alpha = 1.0$. The parameter $p = 0.01$.

We acknowledge the support of National Basic Research Program of China (No. 2006CB705500), the National Natural Science Foundation of China (NNSFC) under Key Project No. 10532060 and Project Nos. 10404025, 70501004, 10672160, 70601026, the CAS special foundation, the Open Project of Key Laboratory of Intelligent Technologies and Systems for Traffic and Transportation, Ministry of Education, Beijing Jiaotong University. R. Wang acknowledges the support of the ASIA:NZ Foundation Higher Education Exchange Program (2005) and Massey Research Fund (2005).

References

1. *Traffic and Granular Flow '99*, edited by D. Helbing, H.J. Herrmann, M. Schreckenberg, D.E. Wolf (Springer, Berlin, 2000); *Traffic and Granular Flow '01*, edited by M. Fukui, Y. Sugiyama, M. Schreckenberg, D.E. Wolf (Springer, Heidelberg, 2003); *Traffic and Granular Flow '03*, edited by S.P. Hoogendoorn, P.H.L. Bovy, M. Schreckenberg, D.E. Wolf (Springer, Heidelberg, 2005); *Traffic and Granular Flow '05*, edited by R.D. Kühne et al., in press
2. B.S. Kerner, *The Physics of Traffic* (Springer, Berlin, New York, 2004)
3. D. Helbing, Rev. Mod. Phys. **73**, 1067 (2001)
4. D. Chowdhury, L. Santen, A. Schadschneider, Phys. Rep. **329**, 199 (2000)
5. T. Nagatani, Rep. Prog. Phys. **65**, 1331 (2002)
6. R. Herman, K. Gardels, Sci. Am. **209**, 35 (1963)
7. D.C. Gazis, Science **157**, 273 (1967)
8. D.C. Gazis, R. Herman, R.B. Potts, Oper. Res. **7**, 499 (1959)
9. L.A. Pipes, J. Appl. Phys. **24**, 274 (1953)
10. R.E. Chandler, R. Herman, E.W. Montroll, Oper. Res. **6**, 165 (1958)
11. E.N. Holland, Transportation Research Part B: Methodological **32**, 141 (1998)
12. X.Y. Zhang, D.F. Jarrett, Transportation Research Part B: Methodological **31**, 441 (1997)
13. M. Bando, K. Hasebe, A. Nakayama, A. Shibata, Y. Sugiyama, Phys. Rev. E **51**, 1035 (1995)
14. M. Bando, K.Hasebe, K. Nakanishi, A. Nakayama, Phys. Rev. E **58**, 5429 (1998); L.C. Davis, Physica A **319**, 557 (2003)
15. H. Ez-Zahraouy, Z. Benrihane, A. Benyoussef, *The Effect Of Delay Times On The Optimal Velocity Traffic Flow Behavior*, e-print `arXvi:cond-mat/0503188`
16. J.M. Del Castillo, P. Pintado, F.G. Benitez, Transportation Research Part B: Methodological **28**, 35 (1994)
17. S. Maerivoet, B.D. Moor, Physics Reports **419**, 1 (2005)
18. K. Nagel, M. Schreckenberg, J. Physique I **2**, 2221 (1992)
19. K. Fourrate, M. Loulidi, Eur. Phys. J. B **49**, 239 (2006)
20. K. Nagel, H.J. Herrmann, Physica A **199**, 254 (1993)
21. K. Nagel, M. Paczuski, Phys. Rev. E **51**, 2909 (1995)